Synthesis and Characterization of Polypropylene/Clay Nanocomposites

JISHENG MA, ZONGNENG QI, YOULIANG HU

State Key Laboratory of Engineering Plastics (SKLEP), Center for Molecular Science, Institute of Chemistry, Chinese Academy of Sciences, Beijing 100080, China

ABSTRACT: Polypropylene/clay (PP/clay) nanocomposites were synthesized via intercalative polymerization. The nanostructure of the composites was investigated by wide-angle X-ray diffractometry (WAXD) and transmission electron microscopy (TEM). The WAXD patterns of the PP/clay nanocomposites indicated that the characteristic diffraction peak of the clay disappeared. The TEM image showed the clay was exfoliated into nanometer size and dispersed uniformly in the PP matrix. The composites exhibited much higher storage modulus compared to that of pure PP. At temperatures higher than T_g, the storage modulus of the PP/clay nanocomposites with 8.1 wt % clay content increased three times that of the pure PP. Additionally, the thermal stability of the nanocomposites significantly increased. The maximum decomposition temperature was increased by 44°C with the introduction of about 10 wt % clay. The heat-distortion temperatures (HDTs) of the nanocomposites also increased. © 2001 John Wiley & Sons, Inc. J Appl Polym Sci 82: 3611–3617, 2001

Key words: PP nanocomposites; montmorillonite; intercalative polymerization

INTRODUCTION

The recent interest in polymer/clay nanocomposites stems from the dramatic improvement in physical properties that can be produced by adding just a small fraction of clay to a polymer matrix.[1] However, the procedure of the polymer/clay preparation was successfully applicable only to polar polymers and not to nonpolar polymers such as polypropylene (PP) that, from a practical point of view, is one of the most widely used polymer materials.[2] Actually, the PP/clay nanocomposites were not obtained even by using a diisoctadecyldimethylammonium-modified clay, in which the polar surfaces of the clay were covered with nonpolar long alkyl chains. Many researchers have recently put forth much effort to solve these problems. Usuki et al.[3–5] reported a PP/clay nanocomposite prepared by a melt intercalative compounding process using a functional oligomer as compatibilizer; however, the introduction of the oligomer reduced the mechanical properties. Oya et al.[6–8] reported the PP/clay nanocomposites prepared through a complicated procedure consisting of three steps; however, the mechanical properties were not improved as they expected.[9] All the reported research works of the PP/clay nanocomposites were focused on the melt intercalative compounding process. However, PP/clay nanocomposites prepared via an intercalative polymerization process have not been found in our literature survey.

In the present study, PP/clay nanocomposites synthesized by intercalative polymerization are reported for the first time. The idea of intercalative polymerization synthesis of the PP/clay nanocomposites is from the concept of a polymerization-filling synthesis of polyolefin composites proposed by D'yachkovskii et al.,[10,11] in which the polyolefin composites were obtained by polymerizing the corresponding monomer on the surface of inorganic filler (e.g., kaolin), which was activated by the Ziegler–Natta catalyst. For the PP/clay nanocomposite of the present work, a layer-structure silicate of Na–montmorillonite was selected as the filler instead of the kaolin. After being modified by intercalative reagent and activated by the Ziegler-Natta catalyst, the activated montmorillonite served as a catalyst for propylene polymerization. During the polymerization, the intercalated propylene monomer in the clay galleries can grow to form the PP macromolecular chains. Because the size of the PP macromolecular chain is far larger than the gallery space, the clay structure would be destroyed and exfoliated by the growing PP molecules. The exfoliated clay building bricks were uniformly dispersed into the PP matrix and had a strong interface between the clay and the PP matrix; thus, the PP/clay nanocomposite produced by this process had better thermal and mechanical properties than that produced by the melt intercalative compounding process. In the present study, the synthesis, structure, and properties of the PP/clay nanocomposites are discussed in detail.

EXPERIMENTAL

Materials

n-Heptane (industrial-grade; Tianjin Chemical Reagent Co., P.R. China) was dried with 4-Å molecular sieves, then refluxed for 24 h over sodium and distilled under nitrogen atmosphere before use. Ethanol (A.R. grade; Tianjin Chemical Reagent Co.) was refluxed for 24 h over magnesium and distilled before use. TiCl$_4$, MgCl$_2$ (Yingkou Science Chemical Co., P.R. China), and triethylaluminum (95% purity; Aybemarle Co., USA) were used without further purification. Propylene (polymerization-grade; Yanshan Petrochemical Co., P.R. China) was used without further purification. Nitrogen (extrapure grade, 99.99% purity) was dried though a P$_2$O$_5$ column. The clay used

was Na–montmorillonite (Na–MMT; Zhangjiakou Qinghe Chemical Factory, P.R. China), whose cation exchange capacity (CEC) was 90–100 mmol/100 g, with a particle size of about 40–70 μm.

Preparation of Organo–Clay

A 5-g sample of Na–montmorillonite was dissolved in 95 g distilled water under a vigorous stirring condition, to form a uniformly dispersed solution, and then 3 g hexadecyl–octadecyl trimethylammonium chloride (intercalative reagent) was added to the solution, which was then stirred for 1 h at 80°C. The dispersed solution was filtered and repeatedly washed with distilled water to remove the excess intercalative reagent, that is, until there was no white precipitate observed in the wash water testing by a 0.1 mol/L AgNO$_3$ solution. The product was then vacuum-dried to a constant weight and ground into powder (diameter about 40–60 μm) to get the organo–montmorillonite (organo–clay).

Activation of Organo–Clay

Before activation, the organo–clay was dried in vacuum at 100–110°C for 10 h; 15 g dried organo–clay and 5 g MgCl$_2$ were then ground together in a vibratory mill for 24 h. The slurry was obtained by mixing the treated organo–clay and MgCl$_2$ in toluene (50 mL). A certain amount of internal electron donor was introduced if needed. TiCl$_4$ (50 mL) was then dropped into the slurry (10 g), with stirring, at the temperature of 100°C for 2 h. Finally the mixture was washed at least five times by n-heptane and dried in vacuum to obtain the activated clay.

Intercalative Polymerization of Propylene

The dried toluene or n-heptane can be used as reaction medium. The polymerization procedure is described as follows. The nitrogen gas was used to remove the traces of oxygen and moisture, first in the reactor. Then the propylene gas was introduced to replace the nitrogen in the reactor and kept the propylene gas at a constant pressure during the polymerization process. Toluene (500 mL), triethylaluminum (1 g), and external electron donor were then injected into the reactor. After the activated clay (2 g) was introduced into the reaction system, the intercalative polymerization was achieved at the temperature of 70–80°C. Finally, the powder of PP/MMT nanocomposite
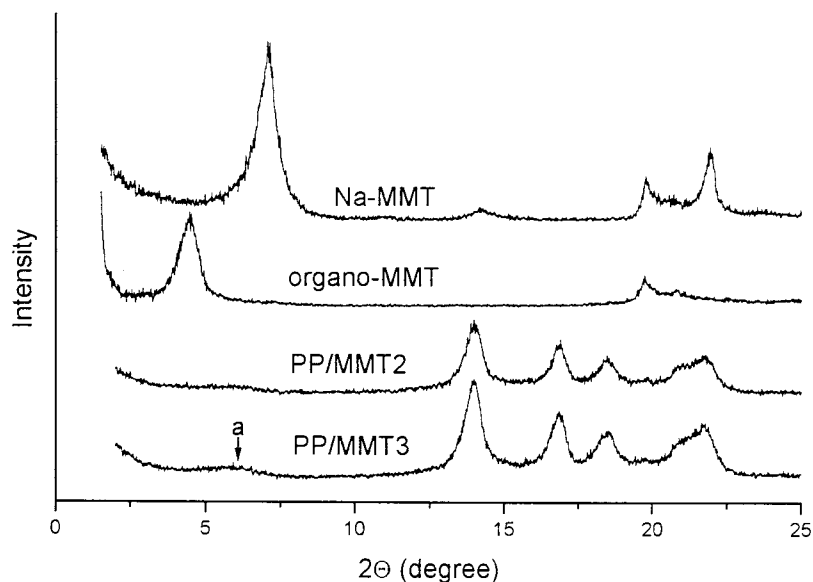
Figure 1 WAXD patterns of organo–MMT and PP/MMT nanocomposites.

product was obtained after terminating, filtering, and drying. The PP/MMT1 (2.5 wt %), PP/MMT2 (4.6 wt %), PP/MMT3 (8.1 wt %), and PP/MMT4 (10.4 wt %) were obtained by controlling the polymerization time. The pure PP was also obtained by using the Ziegler–Natta catalysts without fixing on the clay in the same polymerization condition, for a reference of the PP/clay nanocomposites.

Structure Characterization

A Rigaku (Japan) D/max-RB wide-angle X-ray diffractometer (WAXD) was used to characterize the layer structure of the clay in the nanocomposites. The operation parameters were Cu–K_α radi-

Figure 2 TEM images of PP/MMT nanocomposites.

ation at a generator voltage of 40 kV and current of 100 mA. The scanning rate was 8°/min at an interval of 0.02°. The diffraction intensity was automatically recorded.

The nanometer structure of the nanocomposites was investigated by a Hilaehi (Japan) H-800 transmission electron microscope (TEM) with an acceleration voltage of 100 kV. The ultrathin slides were obtained by sectioning the injection-molded samples along a direction perpendicular to the injection.

Dynamic Modulus Measurement

The dried powder of the nanocomposite was injection-molded into test pieces ($15 \times 2 \times 2$ mm) by a Mini-Max 183 molder (CSI Co., USA) for the measurements of the dynamic mechanical behavior. The dynamic modulus of the nanocomposites was measured by a dynamic mechanical analyzer (DMA-7, Perkin Elmer Cetus Instruments, USA). The dynamic temperature spectra of the nanocomposites were obtained in three-point bending mode at a vibration frequency of 1 Hz in a nitrogen atmosphere, with a temperature range from -50 to 160°C at a scan rate of 5°C/min.

Thermal Behavior Measurement

The thermal stability was measured by thermal gravity analysis (TGA; Perkin–Elmer 7 Series; Perkin Elmer Cetus Instruments, Norwalk, CT) at a scan rate of 20°C/min in nitrogen atmosphere. The heat distortion temperature (HDT)
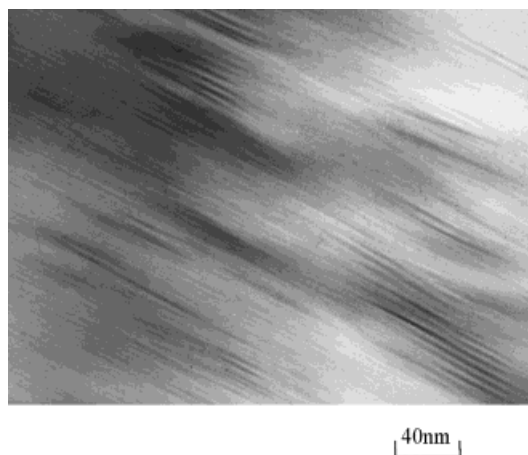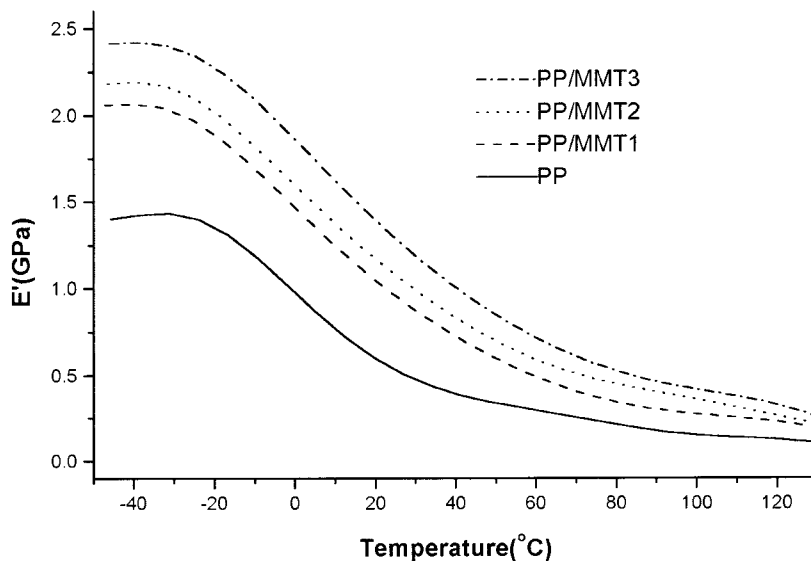
Figure 3   Dynamic storage modulus (E') of PP and PP/MMT nanocomposites.

was taken from the storage modulus versus temperature curves of the dynamic mechanical temperature spectra. According to ASTM D-648, HDT can be defined as such a temperature when the flexural modulus of the sample is 145 MPa.

RESULTS AND DISCUSSION

Layer Structure of the Clay in the PP/Clay Nanocomposites

A nanocomposite is defined as such a composite with the particle size of the disperse phase less than 10^2 nm at least in one dimension.[12] The average diameters of the clay used were about 50 μm and the size of the organo–clay galleries was about 2 nm. Therefore, the small propylene molecules were easily able to enter the organo–clay galleries. According to the intercalative polymerization mechanism, during the polymerization, the small propylene molecules in the galleries grow to form the polypropylene macromolecules. The size of the PP macromolecular chain was about several hundredths of a nanometer, far larger than the gallery space of the clay. Therefore, the layered structure of the clay was de-
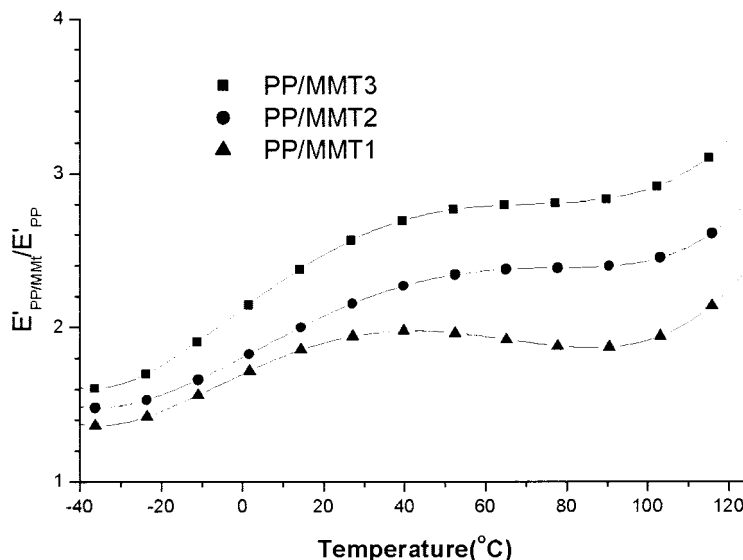

Figure 4   Relative dynamic storage modulus (E'_{co}/E'_{PP}) as a function of temperature.

Table I   Effect of the Clay Content on E', T_g, and HDT of PP/Clay Nanocomposites

	E' (GPa)				T_g (°C)	HDT (°C)
Samples	−40°C	20°C	80°C	120°C		
PP	1.42	0.38	0.21	0.12	6.2	110
PP/MMT1 (2.5 wt %)	2.08	0.76	0.36	0.24	12.1	138
PP/MMT2 (4.6 wt %)	2.22	0.82	0.46	0.28	9.0	144
PP/MMT3 (8.1 wt %)	2.43	0.98	0.54	0.36	8.0	151

stroyed by the growing PP macromolecular chains and uniformly exfoliated in the PP matrix. The evidence of the proposed mechanism is provided by WAXD results. Figure 1 shows the WAXD patterns of the Na–MMT, organo–MMT, and the PP/MMT nanocomposites. The Na–MMT and organo–MMT display their characteristic peaks at $2\theta = 7.12°$ and $4.58°$, respectively, corresponding to the (001) diffraction of layer structure of the Na–MMT and organo–MMT, respectively. However, the characteristic peak disappears in the WAXD pattern of the PP/MMT2 with the clay content of 4.6 wt %, as shown in Figure 1, suggesting that the gallery distance of MMT in the nanocomposite is not less than 8.8 nm (corresponding to $2\theta = 1.5°$), which is the limit of the WAXD used in this study. At such a gallery distance, a nanocomposite is commonly considered as an exfoliated nanocomposite.[13] These results indicate that the propylene molecules intercalate into the clay galleries and destroy the layer structure of the clay, as we mentioned earlier. The WAXD pattern of the PP/MMT3

with the clay content of 8.1 wt % showed a much smaller and broader diffraction peak at about $2\theta = 6.08°$ (shown in Fig. 1, arrow a). This could be attributed to the aggregation of small-portion clay layers when the clay content is more than 8 wt %.

TEM Observation

To study the nanostructure feature of the PP nanocomposites directly, TEM was used to study the dispersibility of the clay in the PP matrix. Figure 2 shows the TEM image of the PP/MMT2 with the clay content of 4.6 wt %. The dark line represents an individual clay layer, whereas the bright area represents the PP matrix. It can be seen that PP chains have intercalated into the clay layers. The clay layers packed along the main axis direction distort with low angle. The TEM image also shows the packing of clay layers containing about two to seven individual layers. The gallery distance is about 4–10 nm. The width of the packing clay layers is about 8–70 nm. Thus, the PP/clay composite is a nanocomposite according to the definition of Calvert.[12] It can be concluded that the stacked clay layers were exfoliated into nanometer-size layers and uniformly dispersed in the PP matrix during the polymerization.

Dynamic Mechanical Temperature Spectra of PP/Clay Nanocomposites

The storage modulus (E') and temperature (T) spectra of the PP and the PP/clay nanocomposites are shown in Figure 3. The nanocomposites have higher E' values than that of the pure PP over the whole temperature range. To clarify the effect of the clay on the E', the storage modulus of PP/MMT relative to that of pure PP
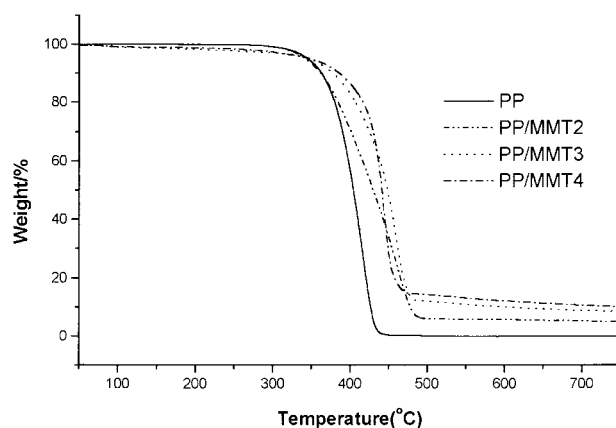
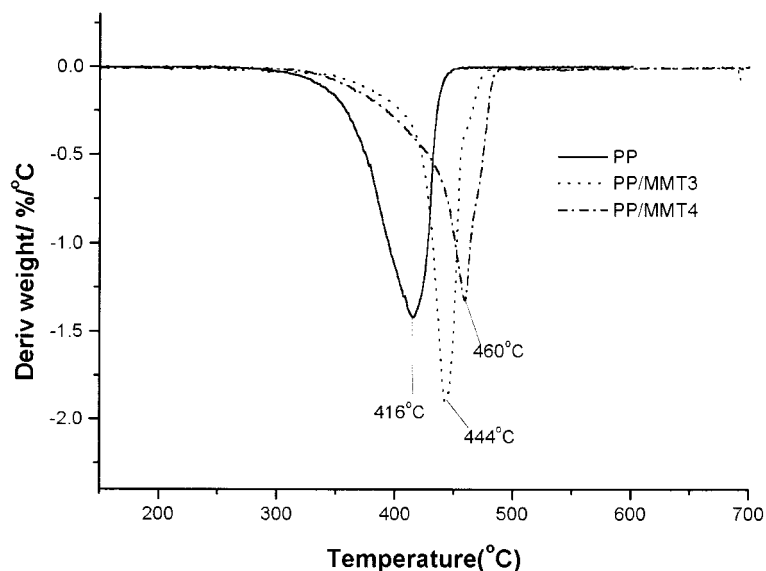**Figure 5**   Thermogravimetric analysis of P and PP/MMT nanocomposites.

Figure 6 Dependency of derivation weight loss on temperature of PP and PP/MMT nanocomposites.

$(E'_{PP/MMT}/E'_{PP})$ was plotted in Figure 4. With increasing clay content, the PP/clay nanocomposites show a substantial increase in E', especially at temperatures higher than T_g. By introducing about 8 wt % clay, the E' is almost three times that of pure PP. The effect of clay content on the E' modulus at -40, 20, 80, and 140°C, respectively; the glass-transition temperature (T_g) taken from the maximum of the loss tangent (tan δ); and the heat-distortion temperatures (HDT) of the PP/clay nanocomposites are listed in Table I.

Thermal Properties of PP/Clay Nanocomposites

The thermal stabilities of the PP/clay and PP studied by TGA analysis are shown in Figure 5. In a comparison of the thermal decomposition temperature of the PP/clay nanocomposites with that of the pure PP, the thermal stability of the nanocomposites is much higher than that of the pure PP. As we can see in Figure 5, the effect of clay on the thermal stability of the nanocomposite is more pronounced. The onset of the thermal decomposition temperature of the nanocomposite was shifted to higher temperatures with increasing clay content. Figure 6 shows the dependency of derivation weight loss on temperature of PP and PP/clay nanocomposites. It shows that, by introducing about 10% clay in the nanocompos-

ites, the temperature of maximum derivative weight loss increased by 44°C over that of the pure PP.

The HDT values of the PP/clay nanocomposites are shown in Table I. The HDTs of the nanocomposites increase with increasing clay content. By introducing about 8 wt % clay, the HDT of the nanocomposite increased by 40°C over that of the pure PP.

CONCLUSIONS

PP/clay nanocomposites were successfully synthesized by intercalative polymerization. The WAXD patterns and TEM image showed that the clay in the nanocomposites was exfoliated into nanometer size and dispersed uniformly in the PP matrix. The storage modulus of the nanocomposites increased with increasing clay content, particularly at temperatures higher than T_g, where the storage modulus was about three times that of the pure PP. The T_g of the nanocomposites increased slightly. The thermal resistance of the nanocomposites was significantly increased. The temperature of the derivative weight loss of PP/MMT (10.4%) was higher than that of pure PP by 44°C. The HDT of PP/clay (8.1 wt %) was increased by 40°C.

REFERENCES

1. Ginzburg, V. V.; Singh, C.; Balazs, A. C. Macromolecules 2000, 33, 1089.
2. Kawasumi, M.; Hasegawa, N.; Kato, M.; Usuki, A.; Okada, A. Macromolecules 1997, 30, 6333.
3. Usuki, A.; Kato, M.; Okada, A.; Kurauchi, T. J Appl Polym Sci 1997, 63, 137.
4. Kato, M.; Okada, A.; Usuki, A. J Appl Polym Sci 1997, 66, 1781.
5. Hasegawa, N.; Kawasumi, M.; Kato, M.; Usuki, A.; Okada, A. J Appl Polym Sci 1998, 67, 87.
6. Furuichi, N.; Kurokawa, Y.; Fujita, K.; Oya, A.; Yasuda, H.; Kiso, M. J Mater Sci 1996, 31, 4307.
7. Kurokawa, Y.; Yasuda, H.; Kashiwagi, M.; Oya, A. J Mater Sci Lett 1997, 16, 1670.
8. Oya, A.; Kurokawa, Y.; Yasuda, H. J Mater Sci Lett 1996, 15, 1481.
9. Oya, A.; Kurokawa, Y.; Yasuda, H. J Mater Sci 2000, 35, 1045.
10. D'yachkovskii, F. S.; Novokshonaova, L. A. Russ Chem Rev 1984, 53, 117.
11. D'yachkovskii, F. S. Trends Polym Sci 1993, 1, 274.
12. Calvert, P. Nature 1996, 383, 300.
13. Kornmann, X.; Lindberg, H.; Berglund, L. A. Polymer 2001, 42, 1301.